Design, Synthesis, and Biological Evaluation of AT_1 Angiotensin II Receptor Antagonists Based on the Pyrazolo[3,4-*b*]pyridine and Related Heteroaromatic Bicyclic Systems

Andrea Cappelli,*[,†] Chiara Nannicini,[†] Andrea Gallelli,[†,‡] Germano Giuliani,[†] Salvatore Valenti,[†] Gal.la Pericot Mohr,[§,†] Maurizio Anzini,[†] Laura Mennuni,[||] Flora Ferrari,[||] Gianfranco Caselli,[||] Antonio Giordani,[||] Walter Peris,[||] Francesco Makovec,[||] Gianluca Giorgi,[⊥] and Salvatore Vomero[†]

Dipartimento Farmaco Chimico Tecnologico and European Research Centre for Drug Discovery and Development, Università di Siena, Via A. Moro, 53100 Siena, Italy, Rottapharm S.p.A., Via Valosa di Sopra 7, 20052 Monza, Italy, and Dipartimento di Chimica, Università di Siena, Via A. Moro, 53100 Siena, Italy

Received September 17, 2007

Novel AT_1 receptor antagonists bearing the pyrazolo[3,4-*b*]pyridine bicyclic heteroaromatic system (or structurally related moieties) were designed and synthesized as the final step of a large program devoted to the development of new antihypertensive agents and to the understanding of the molecular basis of their pharmacodynamic and pharmacokinetic properties. The preliminary pharmacological characterization revealed nanomolar AT_1 receptor affinity for several compounds of the series and a potent antagonistic activity in isolated rabbit aortic strip functional assay for **7c** and **8a**. These results stimulated the study of the biopharmaceutical properties of some selected compounds, which were found to be characterized by a permeability from medium to high. Remarkably, the least permeable **7c** showed both permeability and oral bioavailability (80%) higher than losartan, but its terminal half-life was shorter. These results suggest that the permeability is not a limiting factor in the pharmacokinetics of these AT_1 receptor antagonists.

Introduction

Angiotensin II (Ang II)[a] type 1 (AT_1) receptor belongs to the G protein-coupled receptor superfamily and mediates virtually all the known physiological actions of Ang II through interaction with heterotrimeric G-protein and subsequent activation of several effector systems (phospholipases C, D, A2, adenyl cyclase, etc.). AT_1 receptor shows the seven hydrophobic transmembrane domains forming α-helices in the lipid bilayer of the cell membrane and plays a key role in the renin-angiotensin system involved in the regulation of cardiovascular functions and pathophysiology of hypertension.[1,2]

The discovery of potent and orally active nonpeptide Ang II antagonists such as losartan and eprosartan has encouraged the development of a large number of similar compounds.[3] Among them, irbesartan, candesartan, valsartan, telmisartan, tasosartan, and olmesartan are on the market. Most of the developed AT_1 receptor antagonists are characterized by the presence in their structure of the biphenyl fragment bearing an acidic moiety and differ in the nature of the pendent heterocyclic system (valsartan lacks the heterocyclic moiety) connected to the para position of the proximal phenyl.

The ortho-fused bicyclic imidazo[4,5-*b*]pyridine moiety of compound **2a** (L-158,809) appears to be, from the point of view of the interaction with AT_1 receptor, a particularly effective heterocyclic system.[4] Indeed, this congener of losartan has been reported to show a subnanomolar AT_1 receptor affinity about 1 order of magnitude higher than that of losartan and represents one of the most potent nonpeptide Ang II antagonists so far developed.

On the other hand, irbesartan[5] shows a spirofused bicyclic system, the main axis of which is oriented in a slightly different manner with respect to the corresponding one of compounds **2**. The bicyclic systems of these two compounds are profoundly different from the steric point of view, but each of them shows two potential hydrogen bond acceptors. These results can be considered representative of the widespread information contained in the literature concerning AT_1 receptor antagonists in suggesting that a large variety of heterocyclic moieties is tolerated by the receptor.[6]

At the beginning of an investigation devoted to both the development of new antihypertensive agents and the understanding of the molecular basis of their pharmacodynamic and pharmacokinetic properties, we explored the effects of the molecular manipulation of the distal phenyl group of compounds **2** leading to the development of compounds **4–6**. Some representative compounds of the series showed in vitro properties comparable to those shown by losartan,[7] but pharmacokinetic studies performed with the selected candidates for further preclinical studies revealed low oral bioavailability and a rapid excretion as a possible result of a rapid conjugation with glucuronic acid.[8]

As a further step of the investigation, the structural modification of imidazo[4,5-*b*]pyridine moiety of compounds **2** led to the design of compounds **7** and **8**. In the "recently" described potent AT_1 receptor antagonist **9** the hydrogen bond acceptor imidazole nitrogen of irbesartan is transformed into a pyrazolidinedione carbonyl and the lipophilic spiro-fused cyclopentane moiety is placed between the two carbonyl groups.[9] On the other hand, in compounds **7** and **8** the second potential hydrogen bonding acceptor is incorporated into the lipophilic moiety. In

* To whom correspondence should be addressed. Tel: +39 0577 234320. Fax: +39 0577 234333. E-mail: cappelli@unisi.it.

† Dipartimento Farmaco Chimico Tecnologico and European Research Centre for Drug Discovery and Development, Università di Siena.

‡ Present address: Dipartimento di Scienze Farmacobiologiche, Università degli Studi Magna Græcia di Catanzaro, Complesso Ninì Barbieri, 88021, Roccelletta di Borgia (CZ), Italy.

§ Present address: Medicinal Chemistry, Siena Biotech, Via Torre Fiorentina 1, 53100 Siena, Italy.

|| Rottapharm S.p.A.

⊥ Dipartimento di Chimica, Università di Siena.

[a] Abbreviations: Ang II, angiotensin II; DEM, diethoxymethane; DBU, 1,8-diazabicyclo[5.4.0]undec-7-ene; DMEM, Dulbecco's modified eagle medium.

10.1021/jm7011563 CCC: $40.75
Published on Web 03/05/2008

Scheme 1[a]

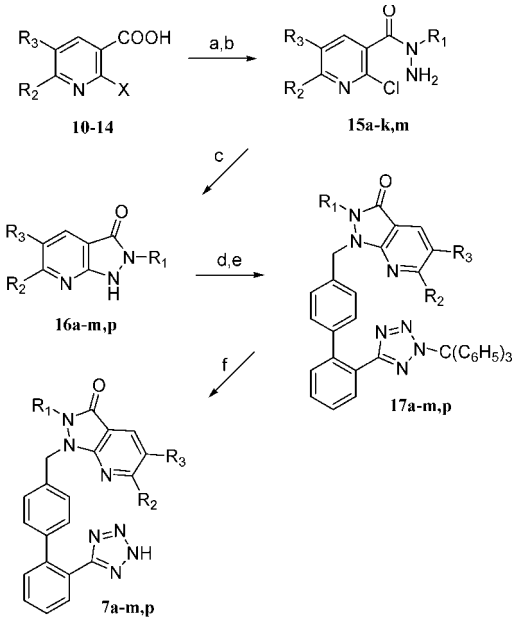

compd	R_1	R_2	R_3
7a	*n*-C_3H_7	H	H
7b	*i*-C_4H_9	H	H
7c	*n*-C_4H_9	H	H
7d	*i*-C_5H_{11}	H	H
7e	*n*-C_5H_{11}	H	H
7f	$CH_2C_6H_5$	H	H
7g	C_2H_5	CH_3	H
7h	*n*-C_3H_7	CH_3	H
7i	*n*-C_4H_9	CH_3	H
7j	*n*-C_4H_9	Cl	H
7k	*n*-C_4H_9	Cl	F
7l	*n*-C_4H_9	H	F
7m	*n*-C_4H_9	H	Cl
7p	*n*-C_4H_9	morpholino	H

[a] Reagents: (a) $SOCl_2$, DMF (cat.); (b) R_1-$NHNH_2 \cdot C_2O_4H_2$, CH_2Cl_2, NaOH, H_2O; (c) 1-pentanol, Na_2CO_3; (d) NaH, DMF; (e) 5-[4′-(bromomethyl)biphenyl-2-yl]-2-(triphenylmethyl)-2*H*-tetrazole, DMF; (f) HCO_2H, CH_2Cl_2.

the design of these compounds the attention was focused on the effects of the orientation of the bicyclic system in order to obtain information useful to refine the previously published AT_1 receptor model.[7]

In this paper the synthesis, the preliminary pharmacological and biopharmaceutical characterization and the deduction of structure−affinity relationships of the novel Ang II antagonists **7** and **8** are described.

Results

Chemistry. The preparation of tetrazole derivatives **7a**−**p** was performed by means of a multistep procedure described in Schemes 1−3.

Scheme 2[a]

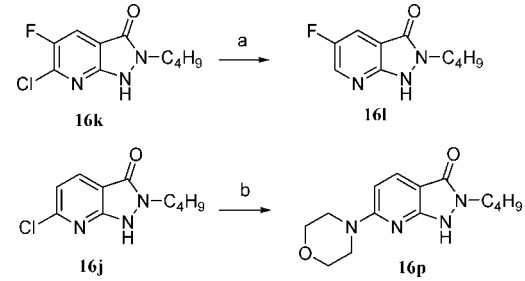

[a] Reagents: (a) H_2, Pd/C, Na_2CO_3, C_2H_5OH; (b) morpholine, C_2H_5OH.

Scheme 3[a]

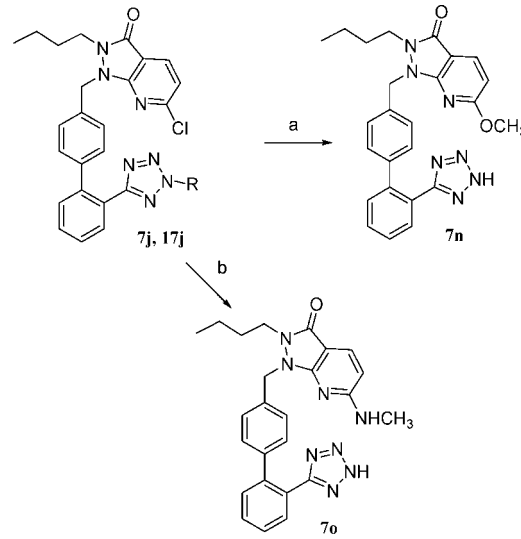

[a] R = H (**7j**), $C(C_6H_5)_3$ (**17j**). Reagents: (a) CH_3ONa, CH_3OH; (b) CH_3NH_2, C_2H_5OH.

The synthesis of pyrazolo[3,4-*b*]pyridine intermediates **16a**−**k**,**m** was accomplished starting from the suitable commercially available nicotinic acids **10**–**14**, which were activated by reaction with thionyl chloride and then made to react with the appropriate hydrazine derivatives to obtain intermediates **15a**−**k**,**m** (Scheme 1). Hydrazide derivatives **15a**−**k**,**m** were then cyclized in refluxing 1-pentanol in the presence of Na_2CO_3 as the base, to give compounds **16a**−**k**,**m**. Moreover, pyrazolo[3,4-*b*]pyridine derivatives **16j**,**k** were used as starting material for the preparation of **16l**,**p** (Scheme 2).

Pyrazolo[3,4-*b*]pyridine derivatives **16** are intriguing compounds, which show prototropic tautomerism. For instance, crystallographic analysis of the two homologues **16a**,**c** show that they crystallize in different prototropic forms characterized by different crystal colors: red prisms in the case of **16a** and colorless needles for **16c** (see Figure 1).

Alkylation of **16a**−**m**,**p** with 5-[4′-(bromomethyl)biphenyl-2-yl]-2-(triphenylmethyl)-2*H*-tetrazole[10] in the presence of NaH as the base gave the expected biphenyl derivatives **17a**−**m**,**p** in acceptable yields, which were deprotected with formic acid to obtain target tetrazole derivatives **17a**−**m**,**p** (Scheme 1). The structure of tetrazole derivative **7a** was confirmed by single crystal X-ray diffraction studies (Figure 2).

The remaining target pyrazolo[3,4-*b*]pyridine **7n**,**o** were prepared by nucleophilic displacement of chlorine atom of **17j** (in the case of **7n**) or **7j** (in the case of **7o**) with sodium methoxide or methylamine, respectively.

Indazolone derivative **18** was prepared by means of the same chemistry described for pyrazolo[3,4-*b*]pyridines **7a**−**m**,**p** with

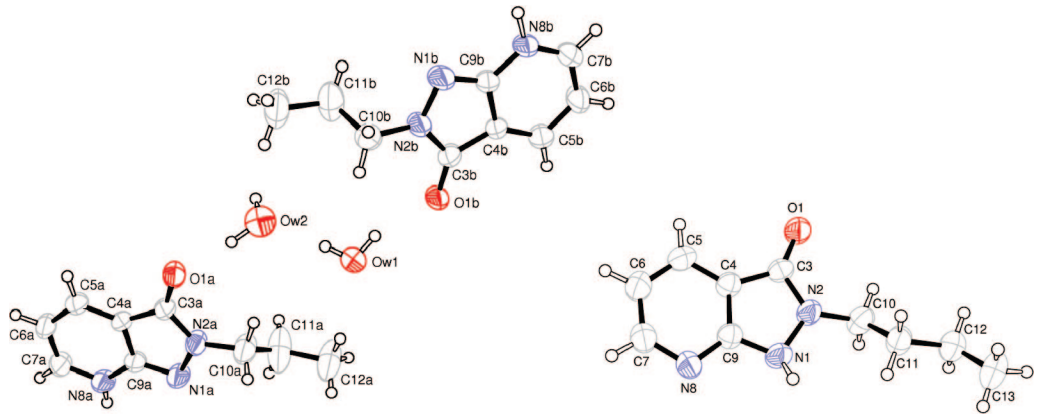

Figure 1. Crystal structure of pyrazolo[3,4-*b*]pyridine derivatives **16a·H_2O** (left) and **16c** (right). Ellipsoids enclose 50% probability.

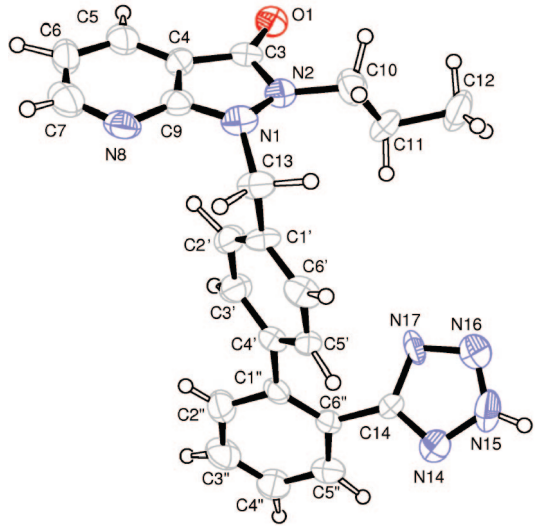

Figure 2. Crystal structure of target compound **7a**. Ellipsoids enclose 50% probability.

the peculiarity that the cyclization of hydrazide derivative **20** was carried out in the presence of a palladium catalyst (Scheme 4).

The target pyrrolo[3,4-*b*]pyridine derivative **7q** (Scheme 5) was synthesized from ethyl 2-methylnicotinate (**23**), which was brominated and cyclized with propylamine to obtain compound **24**, the active methylene of which was acylated with dimethyl carbonate in the presence of sodium hydride as the base to give ester **25**.[11] Compound **25** was deprotonated with sodium hydride in THF and alkylated with 5-[4′-(bromomethyl)biphenyl-2-yl]-2-(triphenylmethyl)-2*H*-tetrazole to give biphenyl derivative **26**, which was promptly deprotected with sodium hydroxide to obtain target tetrazole derivative **7q**.

Target compounds **8a**−**c** were prepared following the multistep procedure described in Scheme 6. The introduction of the required lipophilic side chain in position 1 of the pyrazolo[3,4-*b*]pyridine nucleus was carried out in an indirect manner by reaction of the appropriate ethyl nicotinate derivatives **27**–**29** with the suitable alkylhydrazine to obtain bicyclic compounds **30**–**33**. Crystallographic studies of compounds **30** and **32** showed that these compounds exist in the solid state in the OH-tautomers (Figure 3). Accordingly, alkylation of **30** and **31** with 5-[4′-(bromomethyl)biphenyl-2-yl]-2-(triphenylmethyl)-2*H*-tetrazole in the presence of sodium hydride as the base led to the O-alkylated derivatives **34a**,**b**, which were deprotected to afford the final tetrazole compounds **35a**,**b**. Thus, the preparation of compounds **8a**−**c** required the development of a convergent procedure similar to that described for the synthesis of losartan (Scheme 6).[12]

Scheme 4[a]

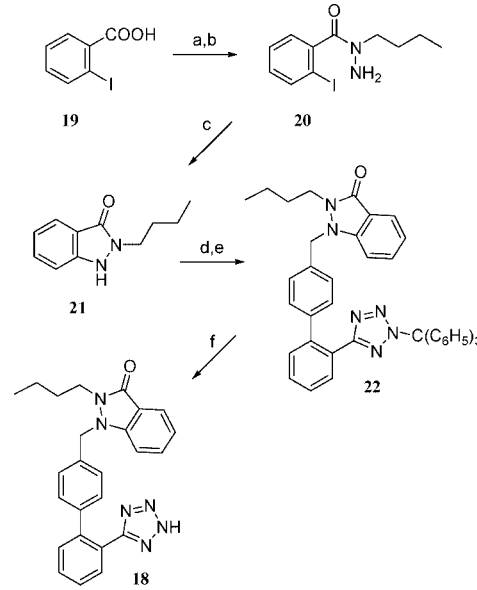

[a] Reagents: (a) $SOCl_2$, CH_2Cl_2; (b) $CH_3CH_2CH_2CH_2$-$NHNH_2 \cdot C_2O_4H_2$, CH_2Cl_2, NaOH, H_2O; (c) NaOH, $Pd(dppf)_2Cl_2$, C_2H_5OH; (d) NaH, DMF; (e) 5-[4′-(bromomethyl)biphenyl-2-yl]-2-(triphenylmethyl)-2*H*-tetrazole, DMF; (f) HCO_2H, CH_2Cl_2.

Pyrazolo[3,4-*b*]pyridine derivatives **31**–**33** were benzylated with 4-bromobenzyl bromide via the corresponding silyl ether derivatives **36a**−**c** to obtain the mixtures of N- and O-alkylated products **37** and **38**, respectively. The expected N-alkylated derivatives **37a**−**c** were isolated from their respective mixtures by flash chromatography (the structure of **37b** was confirmed by crystallography, see the Supporting Information) and subjected to Suzuki coupling reaction with 5-(2′-boronophenyl)-2-(triphenylmethyl)-2*H*-tetrazole[12] to obtain the biphenyl derivatives **39a**–**c**; deprotection with formic acid gave final tetrazole derivatives **8a**–**c**.

Deaza derivatives **8d**–**g** were synthesized starting from ethyl 2-methylnicotinate (**23**) by means of a procedure developed by combining the chemistry[11] used for the preparation of pyrrolo[3,4-*b*]pyridine derivative **7q** with the assembly of the biphenyl moiety based on the Suzuki coupling (Scheme 7).[12] The structure of intermediate compounds **41** and **44d** was confirmed by crystallographic studies (see the Supporting Information).

Scheme 5[a]

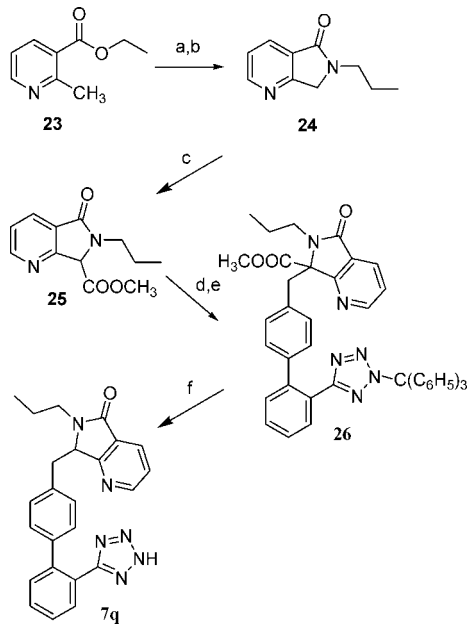

[a] Reagents: (a) NBS, benzoyl peroxide, CCl_4; (b) $CH_3(CH_2)_2NH_2$, C_2H_5OH; (c) $CH_3OCOOCH_3$, NaH, DMF; (d) NaH, THF; (e) 5-[4′-(bromomethyl)biphenyl-2-yl]-2-(triphenylmethyl)-2*H*-tetrazole, THF; (f) NaOH, H_2O, C_2H_5OH.

Finally, the procedure for the synthesis of pyrido[2,3-*d*]pyridazin-8-one derivative **45** is reported in Scheme 8. Condensation of anhydride **46** and butylhydrazine in ethanol afforded compound **47**, which exists in the solid state as the OH-tautomer (see the Supporting Information). Reaction with sodium hydride and subsequently with 5-[4′-(bromomethyl)biphenyl-2-yl]-2-(triphenylmethyl)-2*H*-tetrazole[10] gave the product of O-alkylation **48**, which was deprotected with formic acid to obtain target compound **45**.

Structure−Affinity Relationship Studies. The newly synthesized bicyclic derivatives **7a−q**, **8a−g**, **18**, **35a**,**b**, **45** (showing a suitable degree of purity as confirmed by ^{1}H NMR and combustion analyses) were tested for their potential ability to displace [^{125}I]Sar1,Ile8-Ang II specifically bound to AT_1 receptor in rat hepatic membranes, in comparison with reference compounds **2a**,**b**, losartan, and valsartan, following well-established protocols.[13] The results of the binding studies summarized in Table 1 show that most of the tested compounds displayed submicromolar affinity for AT_1 receptor with the most potent compound **7c** and its positional isomer **8a** showing IC_{50} values in the nanomolar range.

(a) Effects of the Modification of the Heterocyclic System. Among the heterocyclic moieties and their relative orientations with respect to the biphenyltetrazole component investigated in the present work, the pyrazolo[3,4-*b*]pyridine showing a **2a**-like orientation typical of compound **7c** is the most effective configuration from the point of view of the interaction with the AT_1 receptor. However, the difference in affinity between **7c** and **2a** suggests that the carbonyl group of **7c** does not show an optimal geometry for the interaction with the receptor hydrogen-bonding donors (e.g., N111, N294, or S252).[7] A similar conclusion has been drawn in the case of pyrazolidinedione derivative **9**.[9]

The variation in orientation of the pyrazolo[3,4-*b*]pyridine heterocyclic system leading to **8a** has limited effects on the receptor affinity. This result suggests a partial equivalence of the orientations of the pyrazolo[3,4-*b*]pyridine system shown by compounds **7c** and **8a**.

A significant affinity decrease is observed when the heterocyclic system of **8a** is bound to the methylbiphenyltetrazole component by its oxygen atom as it occurs in compounds **35a**,**b**. The introduction of a carbonyl group into the pyrazolo[3,4-*b*]pyridine system of **35b** leading to pyrido[2,3-*d*]pyridazino-8-one derivative **45** has limited effects on the receptor affinity.

The replacement of the pyridine nitrogen atom of **7c** with an aromatic CH group leading to indazolone derivative **18** produces a considerable (33-fold) decrease in the affinity. The result demonstrates the key role played by the pyridine nitrogen in the interaction with the AT_1 receptor.

The transformation of the pyrazolo[3,4-*b*]pyridine heterocyclic system of **7a**,**c** into the pyrrolo[3,4-*b*]pyridine system of **7q** has dramatic effects on the AT_1 receptor affinity. This transformation involves an important center of the molecule, which plays the role of linker between the methylbiphenyltetrazole component and the heterocyclic moiety and affects their relative orientation (Figure 4).

On the other hand, the effect is more limited when the same transformation is carried out in compound **8a** to obtain **8g**. In this case, the transformation involves a linking atom bound to a lipophilic substituent, for which the binding prerequisites are likely to be less stringent.

(b) Effects of the Modification of the Lipophilic Substituent on the Five-Membered Ring. The work performed on losartan congeners has demonstrated the importance of a suitable lipophilic substituent at 2-position of imidazole, fused imidazole, or equivalent moieties in the interaction with the AT_1 receptor. While in the case of losartan derivatives the *n*-propyl and *n*-butyl chains are optimal,[10] in imidazo[4,5-*b*]pyridine derivatives **2**, ethyl and *n*-propyl groups were reported to be equivalent and better than the *n*-butyl one.[4] Interestingly, the *n*-butyl group appears to be the optimal lipophilic substituent in the two short series of pyrazolo[3,4-*b*]pyridine derivatives **7a−f** and **7g−i** and in pyrrolo[3,4-*b*]pyridine derivatives **8d−g**. This result seems to suggest different binding modalities between compounds **2** and our derivatives **7** and **8** probably due to the change of the geometry of the hydrogen bonding acceptor (see Chart 2).

Moreover, the structure−affinity relationship analysis in the series **7a−f** shows that the linear alkyl chains interact with the binding site more tightly than the branched ones (in agreement with the results described for losartan derivatives;[10] compare **7a** with **7b** and **7c** with **7d**) and the benzyl substituent of **7f** is not tolerated at all.

(c) Effects of the Introduction of Substituents on the Pyridine Ring. The introduction of substituents on the pyridine moiety of compound **7c** has negative effects on the affinity for the receptor, and the extent of the affinity decrease depends on the features of the substituent and on the position involved. In fact, a methyl group (**7i**) is better tolerated than a chlorine atom (**7j**), or methoxy (**7n**) and methylamino (**7o**) groups, or again a morpholine substituent (**7p**). Furthermore, the chlorine atom is better tolerated when inserted in position 3 (**7m**) than position 2 (**7j**) of the pyridine ring. Finally, the best accepted substitution pattern appears to be a fluorine atom in position 3 (compound **7l**), while the contemporary presence of the two halogen atoms in positions 2 and 3 of the pyridine ring (**7k**) produces an important affinity decrease.

It is noteworthy that the insertion of either a methyl group (**8b**) or a chlorine atom (**8c**) in the position 2 of the pyridine ring of compound **8a** has negative effects very similar to those observed in compounds **7c**,**i**,**j**. This result suggests a common role for the pyridine ring of compounds **7c** and **8a** in spite of

Scheme 6[a]

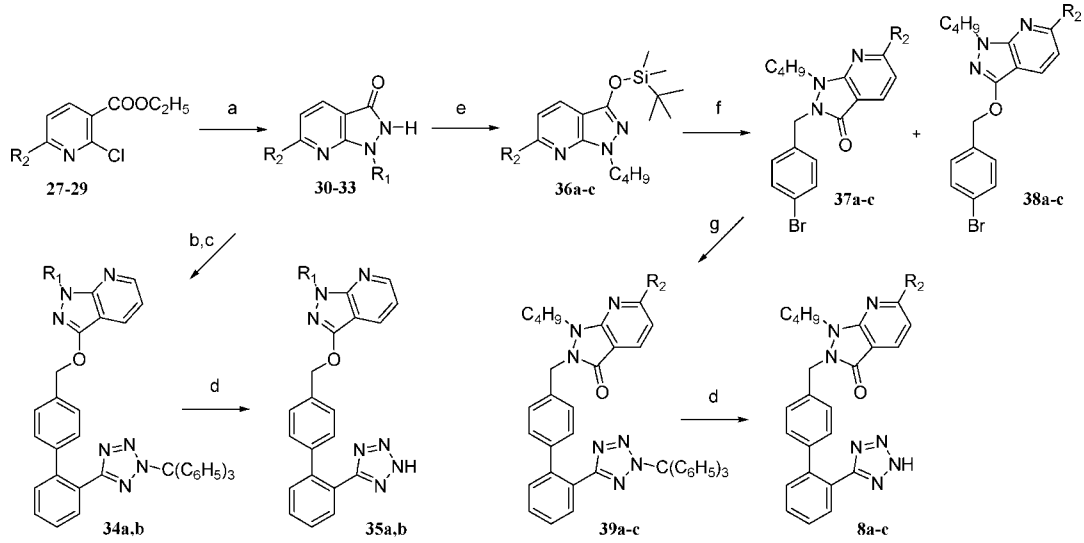

[a] R_1 = *n*-C_3H_7 (**35a**), *n*-C_4H_9 (**35b**); R_2 = H (**8a**), CH_3 (**8b**), Cl (**8c**). Reagents: (a) R_1-NH-NH_2·$C_2O_4H_2$, TEA, C_2H_5OH; (b) NaH, DMF; (c) 5-[4′-(bromomethyl)biphenyl-2-yl]-2-(triphenylmethyl)-2*H*-tetrazole, DMF; (d) HCO_2H, CH_2Cl_2; (e) *tert*-butyldimethylsilyl trifluoromethanesulfonate, *N,N*-diisopropylethylamine, THF; (f) Br-C_6H_4-CH_2Br, (*n*-Bu)$_4$NF, THF; (g) 5-(2′-boronophenyl)-2-(triphenylmethyl)-2*H*-tetrazole, PPh_3, $Pd(OAc)_2$, K_2CO_3, THF, diethoxymethane (DEM), H_2O.

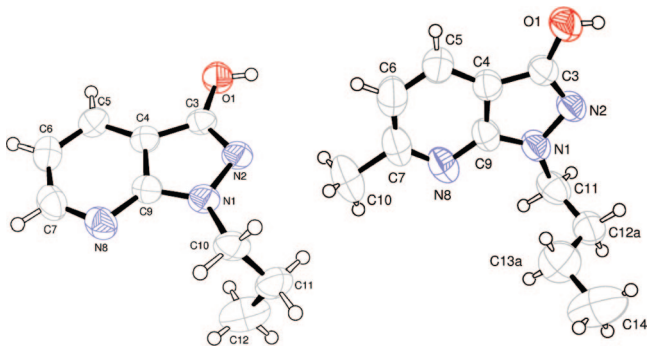

Figure 3. Crystal structure of pyrazolo[3,4-*b*]pyridine derivatives **30** (left) and **32** (right). Ellipsoids enclose 50% probability.

their different orientation with respect to the methylbiphenyltetrazole component.

Functional Studies. The most potent AT_1 receptor–ligands **7c** and **8a** were selected among the newly synthesized compounds and their potential antagonistic activity was investigated in vitro, using the contractile response of isolated rabbit aortic strips as a functional assay. Tissue preincubation with increasing amounts of compounds **7c** and **8a** produced progressive parallel rightward shifts of the endogenous agonist concentration–response curve. Shild's plot analysis gave derived pA_2 values of 7.83 and 7.98 for compound **8a** and **7c**, respectively. Nevertheless, differently from losartan and **7c**, compound **8a** lowered the upper plateau of the concentration–response curve of Ang II in a concentration-dependent way, providing unambiguous evidence for an insurmountable antagonism (Figure 5). This result attains a particular importance in consideration of the fact that **7c** and **8a** are position isomers showing the same pendent heterocyclic system in two different orientations (Chart 2) and suggests that the (in)surmountable antagonist properties can be modulated by very small structural changes in these AT_1 receptor antagonists.

In Vitro Intestinal Permeability Experiments. The permeability studies performed with Caco-2 monolayers[14] show that pyrazolo[3,4-*b*]pyridine derivatives **7c**,**m**, **8a**,**b** and pyrrolo[3,4-*b*]pyridine derivative **8g** are characterized by a medium to high

Scheme 7[a]

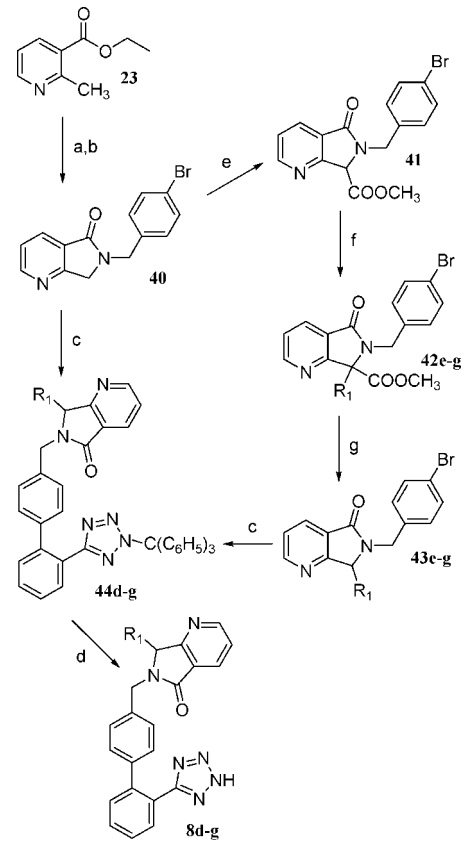

[a] R_1 = H (**8d**), C_2H_5 (**8e**), *n*-C_3H_7 (**8f**), *n*-C_4H_9 (**8g**). Reagents: (a) NBS, benzoyl peroxide, CCl_4; (b) 4-bromobenzylamine hydrochloride, TEA, C_2H_5OH; (c) 5-(2′-boronophenyl)-2-(triphenylmethyl)-2*H*-tetrazole, PPh_3, $Pd(OAc)_2$, K_2CO_3, THF, DEM, H_2O; (d) HCO_2H, CH_2Cl_2; (e) $CH_3OCOOCH_3$, NaH, DMF; (f) DBU, DMF, R_1I; (g) NaOH, H_2O, C_2H_5OH.

permeability in apical to basolateral (A→B) experiments showing P_{app} values ranging from 1.78 to 10.8 × 10^{-6} cm/s (Table 2). For comparison, propanolol shows a P_{app} value of 8.0 × 10^{-6} cm/s in the same test, cimetidine a P_{app} value of 1.1 × 10^{-6} cm/s, and vinblastine (a well-known P-glycoprotein–sub-

Scheme 8[a]

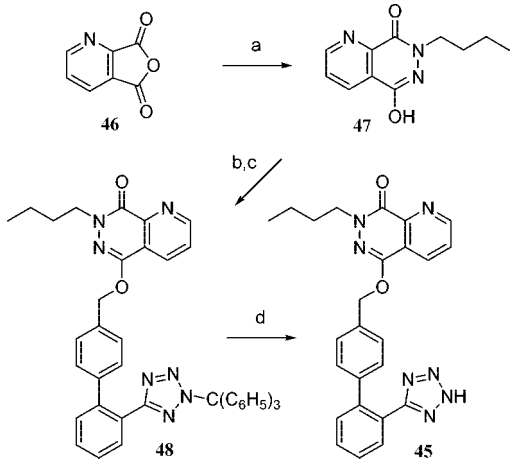

[a] Reagents: (a) $NH_2NHC_4H_9{}^{\bullet}C_2O_4H_2$, TEA, C_2H_5OH; (b) NaH, DMF; (c) 5-[4′-(bromomethyl)biphenyl-2-yl]-2-(triphenylmethyl)-2*H*-tetrazole, DMF; (d) HCO_2H, CH_2Cl_2.

strate) a P_{app} value of 0.1×10^{-6} cm/s. All the newly synthesized compounds show a P_{app} (B→A) value similar to the P_{app} (A→B) value (B→A/A→B ratio < 2, data not shown) suggesting that **7c**,**m**, and **8a**,**b**,**g** are not substrates for efflux. In the short series of the compounds evaluated in such an assay, the least permeable was pyrazolo[3,4-*b*]pyridine derivative **7c**, which shows a P_{app} value slightly higher than those shown by cimetidine and losartan and is about 1 order of magnitude more permeable than the previously described 3-tetrazolylquinolinone derivative **4b** (CR3210, $P_{app} = 0.1 \times 10^{-6}$ cm/s).[8c] The variation in orientation of the pyrazolo[3,4-*b*]pyridine heterocyclic system leading to **8a** has a 2-fold enhancing effect on the permeability, while the introduction of a chlorine atom in position 5 of the pyrazolo[3,4-*b*]pyridine nucleus of **7c** produces a more pronounced enhancing effect, so that **7m** is the most permeable among the compounds tested. On the other hand, the introduction of a methyl group in position 6 of pyrazolo[3,4-*b*]pyridine nucleus of **8a**, as well as the transformation of the pyrazolo[3,4-*b*]pyridine heterocyclic system of **7c** into pyrrolo[3,4-*b*]pyridine one of **7q** slightly improves the permeability. It is noteworthy that the compound showing the highest ClogP (compound **8g**) is not the most permeable, and more in general, the permeability shown by these compounds is apparently poorly related to their lipophilicity.

Pharmacokinetic Studies. The pharmacokinetic properties of compound **7c** were evaluated in rats by standard procedures[8] in comparison with reference AT_1 antagonist **1** (losartan). The results shown in Table 2 suggest that this compound is a chemical entity characterized by very good intestinal absorption and rapid excretion in rats. In fact, pyrazolo[3,4-*b*]pyridine derivative **7c** showed a bioavailability of 80%, but its terminal half-life ranges from 0.9 to 1.0 h.

Discussion and Conclusions

Compounds **7** and **8** were designed as part of a large program devoted to the development of new antihypertensive agents and to the understanding of the molecular basis of their pharmacodynamic and pharmacokinetic properties.[7,8] The designed compounds were synthesized by combining the classical losartan chemistry (linear and convergent approaches) with the chemistry of pyrazolo[3,4-*b*]pyridines and pyrrolo[3,4-*b*]pyridines. Among the newly synthesized bicyclic derivatives, several compounds displayed high affinity for AT_1 receptor. The most potent

Table 1. AT_1 Receptor Binding Affinities of Compounds **2**, **7a**−**q**, **8a**−**g**, **18**, **35a**,**b**, and **45**

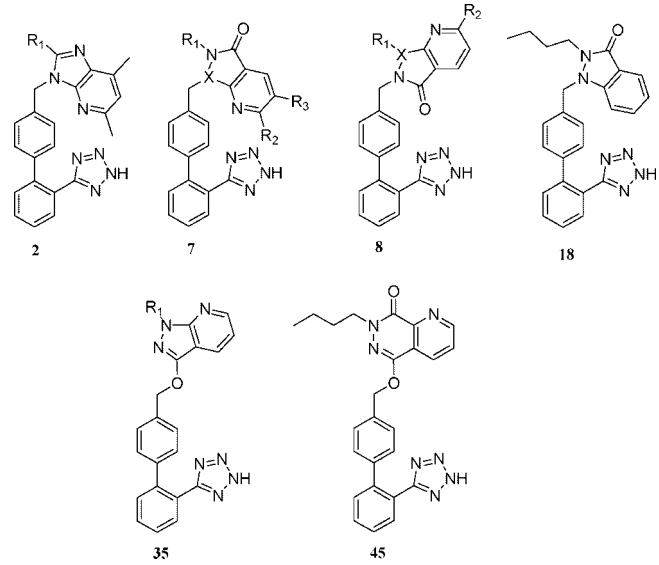

compd	X	R_1	R_2	R_3	binding IC_{50} (nM) ± SEM[a]	rabbit aortic strips pA_2[b]
2a		C_2H_5			0.4 ± 0.1	
2b		*n*-C_3H_7			0.8 ± 0.01	
7a	N	*n*-C_3H_7	H	H	108 ± 18	
7b	N	*i*-C_4H_9	H	H	2300 ± 290	
7c	N	*n*-C_4H_9	H	H	18 ± 1	7.98
7d	N	*i*-C_5H_{11}	H	H	124 ± 8	
7e	N	*n*-C_5H_{11}	H	H	53 ± 4	
7f	N	$CH_2C_6H_5$	H	H	>3000	
7g	N	C_2H_5	CH_3	H	1870 ± 555	
7 h	N	*n*-C_3H_7	CH_3	H	291 ± 29	
7i	N	*n*-C_4H_9	CH_3	H	81 ± 18	
7j	N	*n*-C_4H_9	Cl	H	168 ± 15	
7k	N	*n*-C_4H_9	Cl	F	427 ± 134	
7l	N	*n*-C_4H_9	H	F	70 ± 32	
7m	N	*n*-C_4H_9	H	Cl	76 ± 29	
7n	N	*n*-C_4H_9	OCH_3	H	258 ± 27	
7o	N	*n*-C_4H_9	$NHCH_3$	H	124 ± 16	
7p	N	*n*-C_4H_9	morpholino	H	600 ± 97	
7q	CH	*n*-C_3H_7	H	H	>3000	
8a	N	*n*-C_4H_9	H		39 ± 5	7.83
8b	N	*n*-C_4H_9	CH_3		90 ± 9	
8c	N	*n*-C_4H_9	Cl		461 ± 66	
8d	CH	H	H		>10000	
8e	CH	C_2H_5	H		>10000	
8f	CH	*n*-C_3H_7	H		154 ± 21	
8g	CH	*n*-C_4H_9	H		95 ± 32	
18					598 ± 72	
35a		*n*-C_3H_7			146 ± 33	
35b		*n*-C_4H_9			254 ± 91	
45					114 ± 6	
Ang II					0.4 ± 0.1	
losartan					6.7 ± 0.5	8.48
valsartan					3.4 ± 0.3	

[a] Each value is the mean ± SEM of 3 determinations and represents the concentration giving half-the maximum inhibition of [^{125}I]Sar^1,Ile^8-Ang II specific binding to rat hepatic membranes. [b] The antagonism of Ang II-contracted rabbit aorta strips was assayed by using 60 min as time of contact of the tested compound. Only one curve was obtained from each strip.

compounds **7c** and **8a** show IC_{50} values in the nanomolar range and represent interesting candidates for further preclinical studies. It is noteworthy that compound **7c** and its positional isomer **8a** show quite similar IC_{50} values: 18 and 39 nM, respectively. This small difference finds a support in the literature when **7c** and **8a** are compared with AT_1 receptor

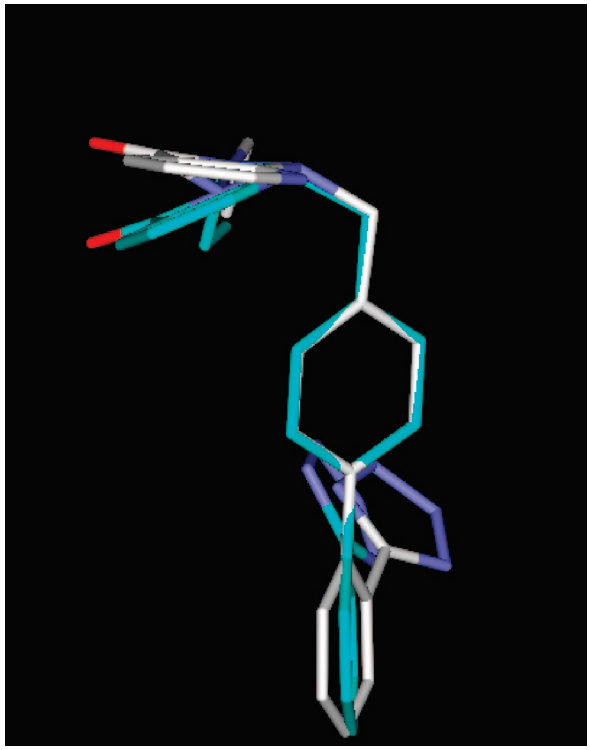

Figure 4. Superposition of **7a** crystallographic structure (white) with a low energy conformer of **7q** (cyan). This result suggests that **7q** can populate the solid state conformation of **7a**. Thus, the difference in the AT_1 receptor affinity between **7a** and **7q** is probably connected to the relative orientation of the pendent bicyclic system determined by the linker geometry (a sp^3 carbon in the case of **7q** and a partially pyramidal nitrogen atom for **7a**).

Chart 1. Structures of Compounds **1**–**6**

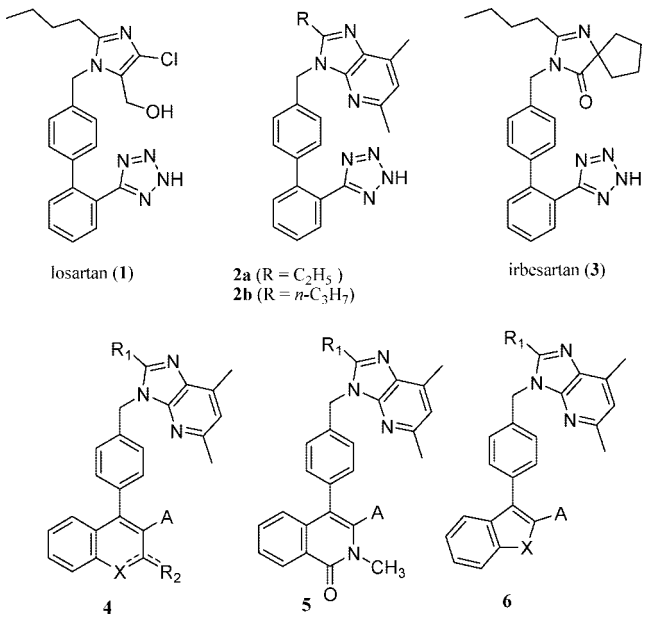

antagonists **9**, **49**, and **50** (Chart 3).[9] The attempts to optimize the interaction with the AT_1 receptor failed to give ligands more potent than **7c** and **8a**, but they afforded several congeners showing interesting affinities and providing valuable information about the interaction with the receptor.

The potential antagonist activity of compounds **7c** and **8a** was investigated in vitro, using the contractile response of isolated rabbit aortic strips as a functional assay. In this test, **7c** was found to behave as a surmountable antagonist, while compound **8a** lowered the upper plateau of the concentration–response curve of Ang II in a concentration-dependent way, providing unambiguous evidence for an insurmountable antagonism. In view of the fact that **7c** and **8a** are position isomers bearing the same pendent bicyclic system in two different orientations, the difference in antagonist behavior suggests that the surmountable/insurmountable antagonist properties can be modulated by very small structural changes.[16]

The results prompted the characterization of the biopharmaceutical properties of some selected compounds. The investigations showed that pyrazolo[3,4-*b*]pyridine derivatives **7c**,**m**, **8a**,**b**, and pyrrolo[3,4-*b*]pyridine derivative **8g** are characterized by a permeability from medium to high and are not substrates for efflux. The least permeable **7c** shows a P_{app} value (1.78×10^{-6} cm/s) slightly higher that shown by losartan and is about 1 order of magnitude more permeable than the previously described 3-tetrazolylquinolinone derivative **4b** ($P_{app} = 0.1 \times 10^{-6}$ cm/s).[8c] Moreover, pharmacokinetic studies showed the high oral bioavailability (80%) of **7c**, which is significantly higher than that shown by losartan and **4b**.[17,8c] The observed differences in bioavailability can be explained on the basis of the different permeability of **7c** and **4b** and by the substantial first-pass hepatic metabolism in the case of losartan.[18,3b]

However, **7c** shows a terminal half-life (about 1.0 h) similar to the one shown by **4b**, but shorter than that of losartan. These results suggest that the permeability is not a limiting factor in the pharmacokinetics of these pyrazolo[3,4-*b*]pyridine derivatives, and further studies are required in order to evaluate the role of UDP-glucuronosyltransferases (EC 2.4.1.17) in the metabolism-excretion of these tetrazole derivatives.[19] In particular, compound **8a** showing nanomolar AT_1 receptor affinity, high permeability, and insurmountable antagonism (which may contribute to the duration of action[20]) can be considered an interesting candidate for further preclinical characterization.

Experimental Section

Chemistry. All chemicals used were of reagent grade. Yields refer to purified products and are not optimized. Melting points were determined in open capillaries on a Gallenkamp apparatus and are uncorrected. Microanalyses were carried out by means of a Perkin-Elmer 240C or a Perkin-Elmer Series II CHNS/O Analyzer 2400. Merck silica gel 60 (230–400 mesh) was used for column chromatography. Merck TLC plates, silica gel 60 F_{254} were used for TLC. ^{1}H NMR spectra were recorded with a Bruker AC 200 spectrometer in the indicated solvents (TMS as internal standard): the values of the chemical shifts are expressed in ppm and the coupling constants (*J*) in Hz. Mass spectra were recorded on either a Varian Saturn 3 spectrometer or a ThermoFinnigan LCQ-Deca.

X-Ray Crystallography. Single crystals of **7a**, **16a**,**c**, **30**, **32**, **37b**, **41**, **44d**, and **47** were submitted to X-ray data collection. Data for compound **41** were obtained by a Bruker-Nonius FR591 rotating anode diffractometer with a 95 mm CCD camera at 120 K. All the other data were obtained by a Siemens P4 four-circle diffractometer at 293 K. Both the instruments were equipped with a graphite monochromated Mo Kα radiation ($\lambda = 0.71069$ Å).

The structures were solved by direct methods implemented in the SHELXS-97 program.[21] The refinements were carried out by full-matrix anisotropic least-squares on F2 for all reflections for non-H atoms by means of the SHELXL-97 program.[22]

Biological Methods. Angiotensin II Receptor Binding Assay. [13] Male Wistar rats (Charles River, Calco, Italy) were killed by decapitation and their livers were rapidly removed. Ang II receptors from rat liver were prepared by differential centrifugation. The liver was dissected free of fatty tissue and minced accurately with small scissors, and about 3 g of tissue was homogenized by Polytron Ultra-Turrax (maximal speed for 2 × 30 s) in ice-cold 20

Chart 2. Structures of Compounds **2a**, **7**–**9**, and Irbesartan[a]

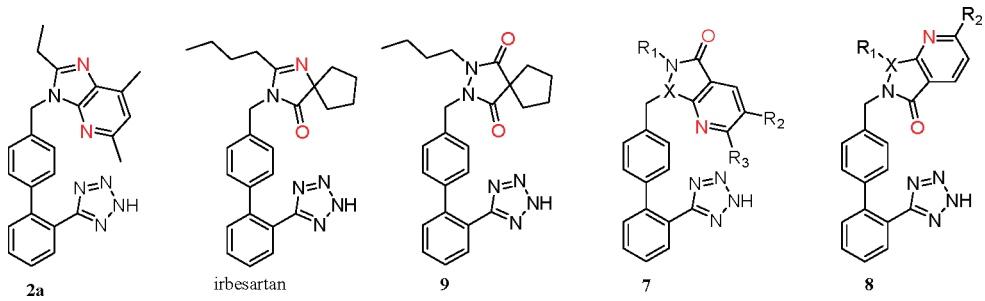

[a] The potential hydrogen bonding acceptors are indicated in red.

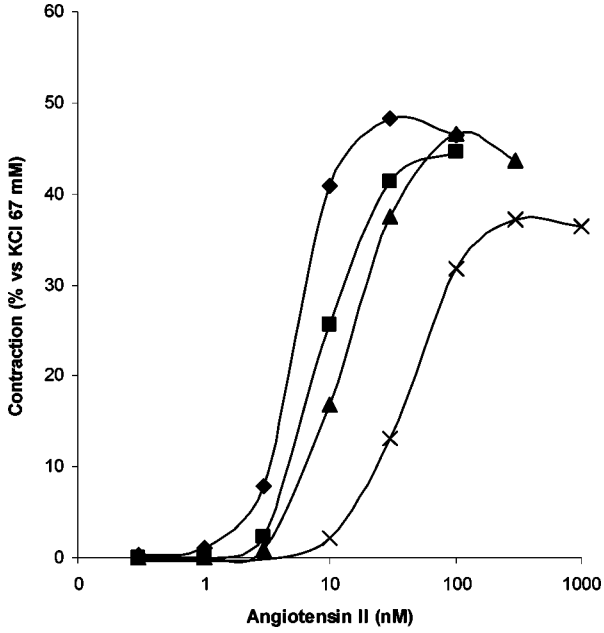

Figure 5. Concentration−contractile response curves for Ang II in isolated rabbit aortic strips, in the presence of different concentrations [10 nM (■), 30 nM (▲), or 100 nM (×)] of compound **8a** or of its vehicle (◆).

vol of Tris-HCl 5 mM, sucrose 0.25 M (pH 7.4). The homogenate was centrifuged at 750*g* for 10 min, and the supernatant was filtered through cheesecloth and saved. The pellets were homogenized and centrifuged as before. The combined supernatants were centrifuged at 50000*g* for 15 min. The resulting pellet was resuspended in Tris−HCl 5 mM, sucrose 0.25 M (pH 7.4) and centrifuged as above. The final pellets were used immediately or stored frozen at −70 °C before use. The membrane pellets were resuspended in the assay buffer (Tris−HCl 50 mM, NaCl 100 mM, $MgCl_2$ 10 mM, EDTA 1 mM, bacitracin 100 μM, PMSF 100 μM, BSA 0.1%, pH 7.4) to obtain a final protein concentration of 0.25 mg/mL. Binding of [^{125}I]Sar^1,Ile^8-Angiotensin II (Perkin-Elmer Life and Analytical Sciences, S.A. 2000 Ci/mmol) to liver membranes was performed at 25 °C for 180 min in 96-well filtration plates (Millipore GFB-Multiscreen). Each 250 μL incubate contained the following: [^{125}I]Sar^1,Ile^8-Angiotensin II (25 pM), liver membrane proteins (25 μg) and standard or test compounds. Nonspecific binding was measured in the presence of 1 μM Ang II and represented 5–10% of total binding. Binding was terminated by rapid vacuum filtration using a Millipore Multiscreen device. Receptor–ligand complex trapped on filters was washed twice with 200 μL of ice-cold NaCl 100 mM, $MgCl_2$ 100 mM. Dried filters discs were punched out and counted in a γ-counter with 92% efficiency. The IC_{50} value (concentration for 50% displacement of the specifically bound [^{125}I]Sar^1,Ile^8-Angiotensin II) was estimated for the linear portion of the competition curves.

Angiotensin II Functional Antagonism in Rabbit Aorta Strips. [13] New Zealand White rabbits (3–4 kg body weight, Harlan Italy) were killed by cervical dislocation, after a slight ether anesthesia. The descending thoracic aorta, with the endothelium removed, was cut into helical strips 3−4 mm wide and 15−20 mm long. These strips were mounted in 20-mL tissue baths containing Krebs−Henseleit solution of the following composition (mM): NaCl 118; KCl 4.69; KH_2PO_4 1.17; $MgSO_4 \cdot 7H_2O$ 1.17; $CaCl_2 \cdot 2\ H_2O$ 2.51; $NaHCO_3$ 25; glucose 11.1. The tissue baths were kept at 37 °C and aerated with 95% O_2 and 5% CO_2. Each strip was connected to an isometric transducer (Basile, Italy), and a resting tension of 2 g was applied to the tissues. Changes in isometric tension were displayed on a four-channel pen recorder (Basile, Italy). The tissues were allowed to equilibrate for 1 h and were washed every 10 min. At the beginning of the experiment, a 67 mM KCl solution was administered to check the sensitivity of the preparations as well as to determine their maximal contractile response. After 30 min washout, test substances or their respective vehicles were added. Sixty minutes later, cumulative concentration–response curves of angiotensin II were obtained. Only one curve was obtained from each strip, and the contractile response was expressed as percentage (%) of the maximal contraction achieved with KCl. Curve analysis was performed by using the Allfit[23] program, which calculates lower and upper plateau, slope and agonist EC_{50}, and allows the comparison of two or more curves. Antagonist potency was evaluated by the estimation of pA_2 values.

In Vitro Intestinal Permeability Experiments. The permeability studies were performed with Caco-2 monolayers as described in the literature.[14] Caco-2 cells were cultured in supplemented Dulbecco's modified eagle medium (DMEM) with 10% fetal bovine serum, 1% nonessential amino acids, 10 mM Hepes buffer, and a Pen/Strept mixture (50U penicillin and 50 mg/mL streptomycin) and split at confluence by trypsinization.

For transport studies, 200000 cells/well were seeded onto Millicell 24-well cell culture plates, and after 24 h incubation at 37 °C with 5% CO_2/95% O_2, the culture medium was changed with Enterocyte Differentiation Medium with additives (Becton Dickinson Bioscience), which allows Caco-2 cells to establish within 3 days a differentiated enterocyte monolayer. Transepithelial electric resistance was measured with a Millipore Millicell-ERS instrument and was >1000 ohms.

The transport across the Caco-2 monolayer was determined in two ways: from apical to basolateral side (A→B) by adding a 10 μM solution of the compound in DMEM (1% final concentration of DMSO) to the apical side and from basolateral to apical side (B→A) by adding a 10 μM solution of the compound in DMEM (1% final concentration of DMSO) to the basolateral side; after 2 h incubation period at 37 °C, the basolateral side solution, together with the apical and the starting solutions, was analyzed and quantified by LC−MS/MS (column: Waters X-terra C18, 2.5 μM, 2.5 × 50 mm, room temperature; mobile phase: acetonitrile−water, flow 250 μL/min; interface: ESI positive mode). The experiments

Table 2. Pharmacokinetic Parameters of Compounds **1**, **4b**, **7c**,**m**, and **8a**,**b**,**g**

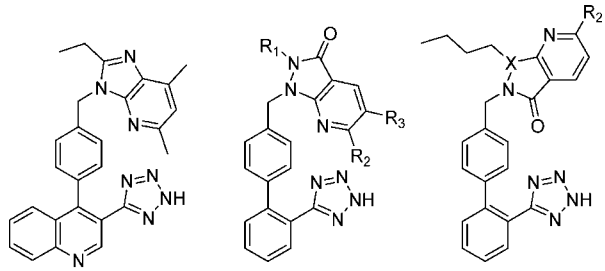

4b **7** **8**

compd	MW	binding IC$_{50}$ (nM)	*C* log *P*[a]	Caco-2 permeability P_{app} (a-b)[b] ($\times 10^{-6}$ cm/s)	dose (mg/kg) (route)	AUC (μg·h/mL)	$t_{1/2}$[c] (h)	C_{max}[d] (μg/mL)	t_{max}[e] (h)	oral bioavail (%)
1 (losartan)	422.91	6.7	4.11[f]	1.15[g]	3 (iv)	12.4	4.7			
					30 (os)	74.8	3.0	27.5	0.5	60
4b	460.53	6.9	4.7	0.10	3 (iv)	0.89	0.68			
					30 (os)	4.40	1.0	4.2	0.5	49
7c	425.49	18	2.95	1.78	5 (iv)	1.41	1.0	6.32		
					15 (os)	3.38	0.9	4.10	0.5	80
7m	459.93	76	3.70	10.8						
8a	425.49	39	2.57	3.6						
8b	439.51	90	3.07	8.7						
8g	424.50	95	4.49	5.6						

[a] *C* log *P* calculated by means of CS ChemDraw Ultra 8.0 (Cambridge Soft Corporation, Cambridge, MA 02140 USA). [b] Apical to basolateral Caco-2 permeability. [c] $t_{1/2}$: terminal half-life. [d] C_{max}: observed maximum concentration after administration. [e] t_{max}: time to reach maximum concentration. [f] For comparison, the log P_{HPLC} value described in the literature was 4.2; see ref 15. [g] See ref 15.

Chart 3. Structures of Compounds **7c**, **8a**, **9**, **49**, and **50**[a]

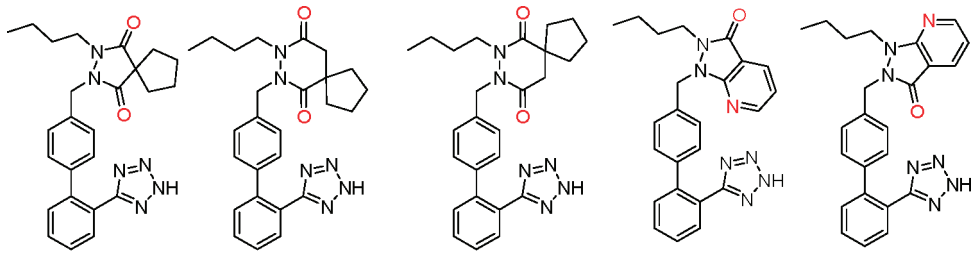

9 K_i = 25 nM **49** K_i = 14 nM **50** K_i = 80 nM **7c** IC_{50} = 18 nM **8a** IC_{50} = 39 nM

[a] The potential hydrogen bonding acceptors are indicated in red.

were performed with buffers at different pH (6.5 apical vs 7.4 basolateral) to better mimic the physiological conditions and propranolol, cimetidine, and vinblastine were evaluated as controls. Caco-2 apparent permeability values (P_{app}) were calculated by means of the following equation:

$$P_{app} = \frac{\Delta Q}{\Delta t}\frac{1}{AC_0} \quad (1)$$

where $\Delta Q/\Delta t$ was the rate of appearance of the drug in the receiver chamber, C_0 was the initial concentration of the drug in the donor chamber, and A was the surface area of the monolayer. All P_{app} values were standardized and reported as 10^{-6} cm/s.

Pharmacokinetics in Rats. Compounds where either orally administered or injected through the tail vein to fasted Sprague–Dawley rats weighing 250–300 g. After the administration, blood samples were taken at selected times and the plasma content was analyzed by HPLC, followed by $t_{½}$ and area under curve calculation (AUC).

Acknowledgment. We thank Prof. Stefania D'Agata D'Ottavi for the careful reading of the manuscript, Dr. Roberto Beretta (Rottapharm, Monza, Italy) for the combustion analyses, and INSTM (Consorzio Interuniversitario Nazionale per la Scienza e la Tecnologia dei Materiali) for the access to Accelrys software. This work was partially supported by MUR (Ministero dell'Università e della Ricerca) - PRIN (Programmi di ricerca di Rilevante Interesse Nazionale).

Supporting Information Available: Full experimental details for the synthesis and the characterization of **7** and **8** and related compounds (chemistry, NMR, MS, crystallography). This material is available free of charge via the Internet at http://pubs.acs.org.

References

(1) De Gasparo, M.; Catt, K. J.; Inagami, T.; Wright, J. W.; Unger, T. International Union of Pharmacology. XXIII. The Angiotensin II Receptors. *Pharmacol. Rev.* **2000**, *52*, 415–472, and references cited therein.

(2) Inoue, Y.; Nakamura, N.; Inagami, T. A Review of Mutagenesis Studies of Angiotensin II Type 1 Receptor, the Three-Dimensional Receptor Model in Search of the Agonist Binding Site and the Hypothesis of a Receptor Activation Mechanism. *J. Hypertens.* **1997**, *15*, 703–714.

(3) (a) Wexler, R. R.; Greenlee, W. J.; Irvin, J. D.; Goldberg, M. R.; Prendergast, K.; Smith, R. D.; Timmermans, P. B. M. W. M. Nonpeptide Angiotensin II Receptor Antagonists: The Next Generation in Antihypertensive Therapy. *J. Med. Chem.* **1996**, *39*, 625–656. (b) Schmidt, B.; Schieffer, B. Angiotensin II AT$_1$ Receptor Antagonist. Clinical Implications of Active Metabolites. *J. Med. Chem.* **2003**, *46*, 2261–2270, and references cited therein.

(4) (a) Mantlo, N. B.; Chakravarty, P. K.; Ondeyka, D. L.; Siegl, P. K. S.; Chang, R. S.; Lotti, V. J.; Faust, K. A.; Chen, T.-B.; Schorn, T. W.;

Sweet, C. S.; Emmert, S. E.; Patchett, A. A.; Greenlee, W. J. Potent, Orally Active Imidazo[4,5-b]pyridine-Based Angiotensin II Receptor Antagonists. *J. Med. Chem.* **1991**, *34*, 2919–2922. (b) Kim, D.; Mantlo, N. B.; Chang, R. S.; Kivlighn, S. D.; Greenlee, W. J. Evaluation of Heterocyclic Acid Equivalents as Tetrazole Replacements in Imidazopyridine-Based Nonpeptide Angiotensin II Receptor Antagonists. *Bioorg. Med. Chem. Lett.* **1994**, *4*, 41–44.

(5) Adams, M. A.; Trudeau, L. Irbesartan: Review of Pharmacology and Comparative Properties. *Can. J. Clin. Pharmacol.* **2000**, *7*, 22–31.

(6) Chakravarty, P. K. Antihypertensive Agents. *Exp. Opin. Ther. Pat.* **1995**, *5*, 431–458.

(7) Cappelli, A.; Pericot Mohr, G.; Gallelli, A.; Rizzo, M.; Anzini, M.; Vomero, S.; Mennuni, L.; Ferrari, F.; Makovec, F.; Menziani, M. C.; De Benedetti, P. G.; Giorgi, G. Design, Synthesis, Structural Studies, Biological Evaluation, and Computational Simulations of Novel Potent AT_1 Angiotensin II Receptor Antagonists Based on the 4-Phenylquinoline Structure. *J. Med. Chem.* **2004**, *47*, 2574–2586.

(8) (a) Rizzo, M.; Anzini, M.; Cappelli, A.; Vomero, S.; Ventrice, D.; De Sarro, G.; Procopio, S.; Costa, N.; Makovec, F. Determination of a Novel Angiotensin-AT_1 Antagonist CR3210 in Biological Samples by HPLC. *Farmaco* **2003**, *58*, 837–844. (b) Rizzo, M.; Ventrice, D.; Monforte, F.; Procopio, S.; De Sarro, G.; Anzini, M.; Cappelli, A.; Makovec, F. Sensitive SPE-HPLC Method to Determine a Novel Angiotensin-AT_1 Antagonist in Biological Samples. *J. Pharm. Biomed. Anal.* **2004**, *35*, 321–329. (c) Cappelli, A.; Pericot Mohr, G.; Giuliani, G.; Galeazzi, S.; Anzini, M.; Mennuni, L.; Ferrari, F.; Makovec, F.; Kleinrath, E. M.; Langer, T.; Valoti, M.; Giorgi, G.; Vomero, S. Further Studies on Imidazo[4,5-*b*]pyridine AT_1 Angiotensin II Receptor Antagonists. Effects of the Transformation of the 4-Phenylquinoline Backbone into 4-Phenylisoquinolinone or 1-Phenylindene Scaffolds. *J. Med. Chem.* **2006**, *49*, 6451–6464.

(9) (a) While this work was in progress, a series of potent AT_1 receptor antagonists based on the pyrazolidine-3,5-dione structure was reported. Le Bourdonnec, B.; Meulon, E.; Yous, S.; Goossens, J.-F.; Houssin, R.; Hénichart, J.-P. Synthesis and Pharmacological Evaluation of New Pyrazolidine-3,5-diones as AT_1 Angiotensin II Receptor Antagonists. *J. Med. Chem.* **2000**, *43*, 2685–2697. (b) Le Bourdonnec, B.; Cauvin, C.; Meulon, E.; Yous, S.; Goossens, J.-F.; Durant, F.; Houssin, R.; Hénichart, J.-P. Comparison of 3D Structures and AT_1 Binding Properties of Pyrazolidine-3,5-diones and Tetrahydropyridazine-3,6-diones with Parent Antihypertensive Drug Irbesartan. *J. Med. Chem.* **2002**, *45*, 4794–4798.

(10) Carini, D. J.; Duncia, J. V.; Aldrich, P. E.; Chiu, A. T.; Johnson, A. L.; Pierce, M. E.; Price, W. A.; Santella, J. B.; Wells, G. J.; Wexler, R. R.; Wong, P. C.; Yoo, S.-E.; Timmermans, P. B. M. W. M. Nonpeptide Angiotensin II Receptor Antagonists: The Discovery of a Series of *N*-(Biphenylmethyl)imidazoles as Potent, Orally Active Antihypertensives. *J. Med. Chem.* **1991**, *34*, 2525–2547.

(11) Anzini, M.; Cappelli, A.; Vomero, S.; Giorgi, G.; Langer, T.; Bruni, G.; Romeo, M. R.; Basile, A. S. Molecular Basis of Peripheral vs Central Benzodiazepine Receptor Selectivity in a New Class of Peripheral Benzodiazepine Receptor Ligands Related to Alpidem. *J. Med. Chem.* **1996**, *39*, 4275–4284.

(12) (a) Larsen, R. D.; King, A. O.; Chen, C. Y.; Corley, E. G.; Foster, B. S.; Roberts, F. E.; Yang, C.; Lieberman, D. R.; Reamer, R. A.; Tschaen, D. M.; Verhoeven, T. R.; Reider, P. J.; Lo, Y. S.; Rossano, L. T.; Bookes, A. S.; Meloni, D.; Moore, J. R.; Arnett, J. F. Efficient Synthesis of Losartan, A Nonpeptide Angiotensin II Receptor Antagonist. *J. Org. Chem.* **1994**, *59*, 6391–6394. (b) Smith, G. B.; Dezeny, G. C.; Hughes, D. L.; King, A. O.; Verhoeven, T. R. Mechanistic Studies of the Suzuki Cross-Coupling Reaction. *J. Org. Chem.* **1994**, *59*, 8151–8156.

(13) (a) Chang, R. S. L.; Siegl, P. K. S.; Clineschmidt, B. W.; Mantlo, N. B.; Chakravarty, P. K.; Greenlee, W. J.; Patchett, A. A.; Lotti, V. J. *In vitro* Pharmacology of L-158,809, a New Highly Potent and Selective Angiotensin II Receptor Antagonists. *J. Pharmacol. Exp. Ther.* **1992**, *262*, 133–138. (b) Robertoson, M. J.; Cunoosamy, M. P.; Clark, K. L. Effects of Peptidase Inhibition on Angiotensin Receptor Agonist and Antagonist Potency in Rabbit Isolated Thoracic Aorta. *Br. J. Pharmacol.* **1992**, *106*, 166–172.

(14) (a) Artursson, P. Epithelial Transport of Drugs in Cell Culture. I: A Model for Studying the Passive Diffusion of Drugs over Intestinal Absorbtive (Caco-2) Cells. *J. Pharm. Sci.* **1990**, *79*, 476–482. (b) Artursson, P.; Karlsson, J. Correlation between Oral Drug Absorption in Humans and Apparent Drug Permeability Coefficients in Human Intestinal Epithelial (Caco-2) Cells. *Biochem. Biophys. Res. Commun.* **1991**, *175*, 880–885.

(15) Ribadeneira, M. D.; Aungst, B. J.; Eyermann, C. J.; Huang, S.-M. Effects of Structural Modifications on the Intestinal Permeability of Angiotensin II Receptor Antagonists and the Correlation of In Vitro, In Situ, and In Vivo Absorption. *Pharm. Res.* **1996**, *13*, 227–233.

(16) Takezako, T.; Gogonea, C.; Saad, Y.; Noda, K.; Karnik, S. S. "Network Leaning" as a Mechanism of Insurmountable Antagonism of the Angiotensin II Type 1 Receptor by Non-peptide Antagonists. *J. Biol. Chem.* **2004**, *279*, 15248–15257.

(17) (a) The marketed AT_1 receptor antagonists show limited oral bioavailability (e. g. eprosartan 13%, valsartan 25%, losartan 33%, candesartan 42%, telmisartan 50%, irbesartan 60–80%. Israili, Z. H. Clinical Pharmacokinetics of Angiotensin II (AT1) Receptor Blockers in Hypertension. *J. Hum. Hypertens.* **2000**, *14* (1), S73–86. (b) Brunner, H. R. The New Angiotensin II Receptor Antagonist, Irbesartan. *Am. J. Hypertens.* **1997**, *10*, 311S–317S. (c) Moreover, losartan exhibiting highly variable oral bioavailability is transported by P-glycoprotein, while its carboxylic acid metabolite is not a P-glycoprotein substrate; see: Soldner, A.; Benet, L. Z.; Mutschler, E.; Christians, U. Active Transport of the Angiotensin-II Antagonist Losartan and its Main Metabolite EXP 3174 Across MDCK-MDR1 and Caco-2 Cell Monolayers. *Br. J. Pharmacol.* **2000**, *129*, 1235–1243.

(18) http://www.fda.gov/cder/foi/label/2002/20386s28lbl.pdf.

(19) (a) Comparative studies on the UDP-glucuronosyltransferase-dependent metabolism showed that intrinsic clearance ($CL_{intrinsic} = V_{max}/K_m$) of compound **4b** is 7-fold higher than that shown by **2a** (Valoti, M. Personal communication). Interestingly, other authors reported that the absence of **2a** glucuronide in the hepatocyte and its presence in the bile suggest that its rate of formation is much slower than that of transport out of the cell [see: Colletti, A. E.; Krieter, P. A. Disposition of Angiotensin II Receptor Antagonist L-158,809 in Rats and Rhesus Monkeys. *Drug Metab. Dispos.* **1994**, *22*, 183–188. (b) Huskey, S. W.; Miller, R. R.; Chiu, S.-H. L. N-Glucuronidation Reactions. I. Tetrazole N-Glucuronidation of Selected Angiotensin II Receptor Antagonists in Hepatic Microsome from Rats, Dogs, Monkeys, and Humans. *Drug Metab. Dispos.* **1993**, *21*, 792–799, and references cited therein].

(20) Vauquelin, G.; Van Liefde, I.; Birzbier, B. B.; Vanderheyden, P. M. L. New Insights in Insurmountable Antagonism. *Fund. Clin. Pharmacol.* **2002**, *16*, 263–272.

(21) Sheldrick, G. M. SHELXS-97, Rel. 97-2, A Program for Automatic Solution of Crystal Structures, Gottingen University, 1997.

(22) Sheldrick, G. M. SHELXL-97, Rel. 97-2, A Program for Crystal Structure Refinement, Gottingen University, 1997.

(23) De Lean, K. W.; Munson, P. J.; Rodbard, D. Simultaneous Analysis of Families of Sigmoidal Curves: Application to Bioassay, Radioligand Assay and Physiological Dose-Response Curves. *Am. J. Physiol.* **1978**, *235*, E97–E102.

JM7011563